Development of novel polyethylene air-cathode material for microbial fuel cells

Ningshengjie Gao [a], Botong Qu [b], Zhenyu Xing [c], Xiulei Ji [c], Eugene Zhang [b], Hong Liu [a, *]

[a] *Department of Biological and Ecological Engineering, Oregon State University, Corvallis, OR, 97331, United States*
[b] *School of Electrical Engineering and Computer Science, Oregon State University, Corvallis, OR, 97331, United States*
[c] *Department of Chemistry, Oregon State University, Corvallis, OR, 97331, United States*

ARTICLE INFO

ABSTRACT

Air-cathode fabrication is currently a key factor that hinders the scaling up of microbial fuel cell (MFC) technology. A new type of cathode material that contains porous polyethylene (PE) sheet and a blended activated carbon (AC) and highly conductive carbon back (CB) layer was developed for the first time. The PE sheet functions as both gas diffusion layer (GDL) and cathode supporting material. The blended AC and CB layer eliminates expensive current collector. Among different types of PE sheets and AC and CB blending ratios, the cathode with Type I PE sheet (75—110 μm pore size) and a CB/AC ratio of 1: 0.5 demonstrated the best performance (8.4 A m^{-2} at 0 V) in electrochemical cells. MFCs with this cathode generated more stable and higher power densities compared with those using PTFE cathodes. Simulation of ohmic potential drops across this cathode material suggests that using a two-parallel terminal connection design would result in only 0.04 V potential drop at 1 m^2 scale. This study suggests that this new PE cathode material has great potential for use in scaled up MFC systems due to its decent performance, simple fabrication process, and use of low-cost material.

© 2018 Elsevier Ltd. All rights reserved.

1. Introduction

Water and energy are two major global challenges. Typical domestic wastewater is rich in energy (1.93 kWh m^{-3}) [1]. Microbial fuel cell (MFC) technology can generate electrical energy from organic materials and has potential applications in wastewater treatment, portable electric devices, and bioremediation [2—6]. In an MFC, exoelectrogenic bacteria degrade organic compounds and generate electrons and protons. The electrons are transferred extracellularly to the anode and flow to the cathode through external circuit [2]. The protons diffuse to the cathode and react with electrons and ultimate electron acceptors, such as oxygen, ferricyanide and manganese dioxide [7—9]. Oxygen is the most frequently-used electron acceptor for its universal availability. Cathodes using dissolved oxygen have been explored in some up-flow reactors [10—13], but due to the extra energy input for aeration and the relatively low power output [7,14—16], most of the recent studies used air-cathodes, which are directly exposed to the air [2,17].

Many recent advances have been made to enhance the performance of air-cathode MFCs. Reducing internal resistance is one of the key efforts to increase the power output of MFCs, which can be achieved through using closer electrode distance [18—21]. Efforts have also been made on increasing the total volumetric electrode surface area [19,21—25] and enhancing hydraulic conditions in reactors [26,27]. Some new membrane/separator materials were also investigated to enhance the proton conductivity and anti-fouling property and lower the cost [15,28—30]. However, further enhancement of these systems will rely on the improved cathode material [18,31]. Developing a stable, low-cost, and scalable air-cathode is the key challenge for successful application of MFC technology for various applications, especially in wastewater treatment [18].

An air cathode typically contains a catalyst layer, a current collector/supporting layer, and a gas diffusion layer (GDL). Carbon-based materials such as activated carbon (AC) are more favored than platinum as catalyst due to their decent performance and low cost [4,19,32,33]. Metals and carbon based current collectors can reduce the electrode resistance during electrons transfer through the electrode and can also provide mechanical support for the cathode [4,19,23,32—34]. However, stainless steel and nickel based

* Corresponding author.
 E-mail address: hong.liu@oregonstate.edu (H. Liu).

Abbreviations		$U(x, y)$	potential on each simulated point
		(a_i, b_i)	the neighbor points of (x, y)
AC	activated carbon	k	the total number of the neighbor points (i.e. 2, 3, or 4)
CB	carbon black	I	the total current
CC	carbon cloth	R	the calculated resistance of each point ($1\ mm \times 1\ mm$ unit)
CE	coulombic efficiency		
EIS	electrochemical impedance spectroscopy	R_0	the measured resistance of the catalyst layer
GDL	gas diffusion layer	ρ	resistivity
LSV	linear sweep voltammetry	S	the cross-sectional area of the stainless steel rod
MFC	microbial fuel cell	L	the thickness of the measured catalyst layer after the press
PE	polyethylene		
PTFE	poly(tetrafluoroethylene)	R_d	diffusion resistance
SSM	stainless steel mesh	W	Warburg impedance
PEMFC	proton exchange membrane fuel cell	R_{ct}	charge transfer resistance
du	constant potential drop on each simulated point		

current collectors have been reported to be corroded over time and resulted in performance decrease [35,36]. Carbon cloth (CC) is conductive and corrosion-resistant. However, additional supporting layers may be needed for scale-up MFCs due to its soft and fibrous nature. GDL, which is typically jointed with current collector, functions as water barrier and oxygen diffuser. Many polymers, such as poly(tetrafluoroethylene) (PTFE), poly(dimethylsiloxane) (PDMS) and poly(vinylidene fluoride) (PVDF), have been used to form the GDLs of cathodes [37—41].

Simplifying the GDL fabrication process is currently the key for air cathode scaling up. The polymers mentioned above either need to be cured at high temperature, or have relatively complex fabrication process [37—41]. PTFE emulsion, the most commonly used material for making air-cathode GDL, is typically first painted on the supporting layer/current collector such as CC and stainless steel mesh (SSM) and then heated at 370 °C to form multiple PTFE layers [33,37]. Rolling method has also been used to roll down the CB and PTFE mixture onto SSM in order to simplify the cathode fabrication. Yet, high temperature of 340 °C is still needed to cure the PTFE [4,41]. Other polymer solutions, such as PDMS and PVDF, have also been used to form air-cathode GDL at low temperature. However additional solvents, such as toluene and N, N-dimethylacetamide (DMAc), were used to dilute the polymer solution [38,39], which could increase the overall fabrication cost. Some waterproof and air-permeable fabric/membranes, such as GORE-TEX cloth and PVDF membrane have also been investigated as GDL [40,42,43]. However, current collector/supporting layer was still needed due to the low mechanical strength of the materials.

In this study, a new air cathode material was developed that uses rigid and porous polyethylene (PE) sheet as GDL and mechanical support for the first time. This new cathode material was evaluated in both electrochemical cells and lab MFCs. Highly conductive carbon black (CB) was blended with AC catalyst at various ratios to investigate the impact of conductivity on the performance. Simulations of ohmic potential drop, a parameter that reflects the potential decrease due to material resistance, across the electrode were also implemented to evaluate the scaling up potential of this new material.

2. Materials and methods

2.1. Cathode fabrication

Three types of PE sheets (Porex Corp., USA) with different properties (Table 1) were investigated for their feasibility of being used as MFC cathode GDL and supporting layer. The cross-section

Table 1
Characteristics of the tested PE sheets.

	pore size (um)	thickness (mm)	air flow rate (mL min^{-1} cm^{-2})[a]
type I	75—115	0.53—0.74	790—1580
type II	90—160	1.32—1.83	849—1185
type III	50—90	1.50—2.00	296—691

[a] Air flow values are measured at inlet pressure of 3 cm water.

and surface morphology of the PE sheets was examined using scanning electron microscope (SEM) (Quanta 600F, FEI, USA). A catalyst mixture was prepared by first mixing AC (Charcoal House, USA) and CB powder (XC-72R) at different mass ratios (1:1, 1:0.5, 1:0.25, 1:0.17, and 1:0.1). The AC loading was kept at 25 mg cm^{-2} for all cathodes. PTFE emulsion (60%, Dupont, USA) was then added as binder (0.2 mL g^{-1} total carbon) to form a catalyst paste. The paste was applied evenly onto one side of the PE sheet and pressed by a roller (Figure S1). PTFE-CC cathodes with the same AC and PTFE loadings (AC/CB ratio of 1:0.1) were fabricated as previously described for comparison [36].

2.2. Cathode evaluation in electrochemical cells

The fabricated cathodes were evaluated in electrochemical cells by linear sweep voltammetry (LSV) using a potentiostat (CHI 1000C, CH Instruments, Inc.). The electrochemical cells were made of two cylindrical chambers separated by a Nafion membrane with an empty bed volume of 14 mL for each chamber (2 cm long and 7 cm^2 cross-sectional area). Each electrochemical cell contained a Pt plate (2.5×2.5 cm^2) counter electrode, a Ag/AgCl reference electrode, and a working electrode (0.7 cm^2 cathode sample). The reference electrodes were made with curly tip to reduce the distance between the reference and working electrode [33]. The small working electrodes can reduce the surface area to volume ratio and minimize the influence of H$^+$ consumption during the test [16]. LSV experiments were conducted at a potential window of -0.2—0.3 V (vs. Ag/AgCl) at a scan rate of 0.1 mV s^{-1} and room temperature. The final curves were chosen when the two consequence scans were well overlaid.

Electrochemical Impedance Spectroscopy (EIS) was performed in electrochemical cells using a potentiostat (VMP3, BioLogic, USA). The electrochemical cell has the same dimension as previously mentioned, but with a Pt wire reference electrode and without Nafion membrane. The EIS was carried out in a frequency range of 100 kHz—10 mHz at open circuit potential with an AC voltage of

10 mV. The data were then interpreted according to an equivalent circuit [44]. The electrolyte (pH = 7) contains (per liter): KCl, 0.13 g; NH$_4$Cl, 0.31 g; NaH$_2$PO$_4$·H$_2$O, 2.92 g; Na$_2$HPO$_4$, 4.1 g [2]. The electrolyte was purged with N$_2$ gas to remove the dissolved oxygen prior to the test, and was replaced by new and purged electrolyte between scans.

2.3. MFC construction and operation

The cathodes were also evaluated in single-chamber MFCs. The MFCs were assembled as previously described [2] with both anode and cathode surface area of 7 cm^2 and total volume of 14 mL. Two Ti wires were fixed on both sides of the cell chamber and used for connecting the electrodes with the external circuit. The contact area between the wire and the electrode were referred as terminals for electron flow. All MFC were inoculated with an exoelectrogenic culture scratched from pre-acclimated MFC anodes that had been fed with sodium acetate under fed-batch mode over 12 months. The MFCs were operated at cell voltage around 0.33 V with an external resistance between 100 and 130 Ω to maintain the max power output. The performance of the PE cathodes was also compared with the PTFE cathode in the MFCs with the same anodes that had mature biofilms. The electrolyte was the same solution used in the electrochemical tests with the addition of sodium acetate (80 mM), minerals and vitamins for bacteria growth [2,45]. All MFCs were operated in fed-batch mode in a temperature control chamber (30 ± 1 °C). The medium solution was replaced with new medium when the voltage was below 0.03 V. Coulombic efficiency (CE) was determined using total coulombs recovered as electricity divided by the total coulombs contained in the substrate (sodium acetate) following a previous study [46]. Voltages were continuously recorded by a data acquisition system (2700, Keithly, USA).

2.4. Electrode resistance measurement and scaling up simulation

The conductivity of electrode is typically not a concern when the electrode size or current is small. However, with the increase of electrode size and current, significant potential drop can occur due to the long distance traveling of electrons from the terminal to electrode surface [47]. Since the conductivity of the PE cathode was determined by the ohmic resistance of catalyst layer (the only conductive layer on the cathode), ohmic resistance of the catalyst layer was measured for scaling up simulation. The catalyst was first pressed between two stainless steel rods with an insulated Swagelok at 180 MPa and then its resistance (R_0) was measured by a source meter. The resistivity (ρ) was calculated by

$$\rho = R_0 \times \frac{S}{L} \tag{1}$$

where R_0 is the measured resistance, S is the cross-sectional area of the stainless steel rod, and L is the thickness of the measured catalyst layer after the press.

Scaling up simulations on potential drop across the catalyst layer were conducted based on the following assumptions: 1) the potential drop is the difference between the terminal and a random spot on the catalyst surface; 2) the catalyst layer is a 2D surface and can be divided into 1 mm × 1 mm units, which are represented by points; 3) each point is only connected with surrounding 2 to 4 orthogonal points; 4) only ohmic resistance of the catalyst layer contributes to the potential drops; 5) the catalyst layer has uniform properties, so the current output is evenly distributed to all points; 6) the current density is 3 A m^{-2}; 7) potentials at the Ti wire connecting terminals are set to be 0 V. Six different terminal designs were chosen to compare the potential drop under these conditions.

The potential of a particular point depends on the resistance and current according to the Ohm's law. For a particular point, the total current that flows in equals to the total current that flows out. Therefore, each point's potential equals to the average of the surrounding points' potential minus a constant potential drop (du).

At terminal points set T (T_1, T_2, …, T_n), the potentials were set to be 0 V. For each point (x, y), its potential $U(x, y)$ was calculated by averaging the potentials of the neighbor orthogonal points following equation (2) (examples of calculation were provided in SI, equations S1-S3):

$$U(x,y) = \begin{cases} \dfrac{1}{k} \displaystyle\sum_{i=1}^{k} U(a_i, b_i) - du, & if \ (x, y) \notin T \\ 0, & if \ (x, y) \in T \end{cases} \tag{2}$$

Where (a_i, b_i) are the neighbor points of (x, y), k is the total number of the neighbor points (i.e. 2, 3, or 4), and du is the constant potential drop on each point $du = I \times R/(size)^2$. I is the total current (A), size refers to the length of the simulated cathode in a unit of millimeter (mm), and R is the resistance of each point, which was calculated to be 0.0868 Ω (AC/CB = 1:0.5).

A sparse matrix was constructed by considering all points as the variables of the linear equation system (equations S4-S7). The calculation results were then visualized in Matlab. Simulation with different cathode surface areas (0.1 m × 0.1 m, 0.5 m × 0.5 m, and 1 m × 1 m) were compared.

3. Results and discussion

3.1. Selection of PE sheet

Three types of porous PE sheets were evaluated to compare the impacts of different sheet properties on the cathode performance (Fig. 1). Cathode with type I PE sheet achieved the highest current density (8.4 A m^{-2}) at 0 V (vs. Ag/AgCl) compared with type II (8.0 A m^{-2}) and type III (6.7 A m^{-2}). The relatively low performance of type III PE sheet cathode is possibly due to the lower air flow rate, which affects the oxygen transfer to the catalyst layer (Table 1). This can also be seen from the SEM images (Fig. 2) that type III had uneven particle sizes and the particles not well connected. With similar air flow rates, type I and type II PE sheet achieved comparable performance at lower potential (−0.2 V−0 V). However, type I demonstrated better performance at higher potential (0 V−0.3 V) possibly due to the more uniform and finer particle size than type II. Therefore, type I PE sheet was selected for further evaluation.
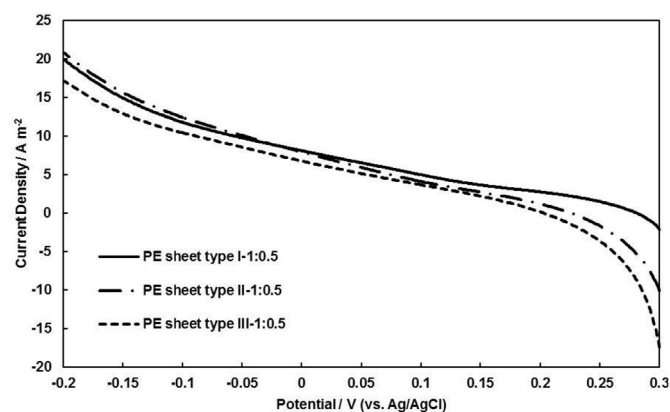

Fig. 1. Performance of PE cathodes with different types of PE sheet at AC/CB ratio of 1:0.5.
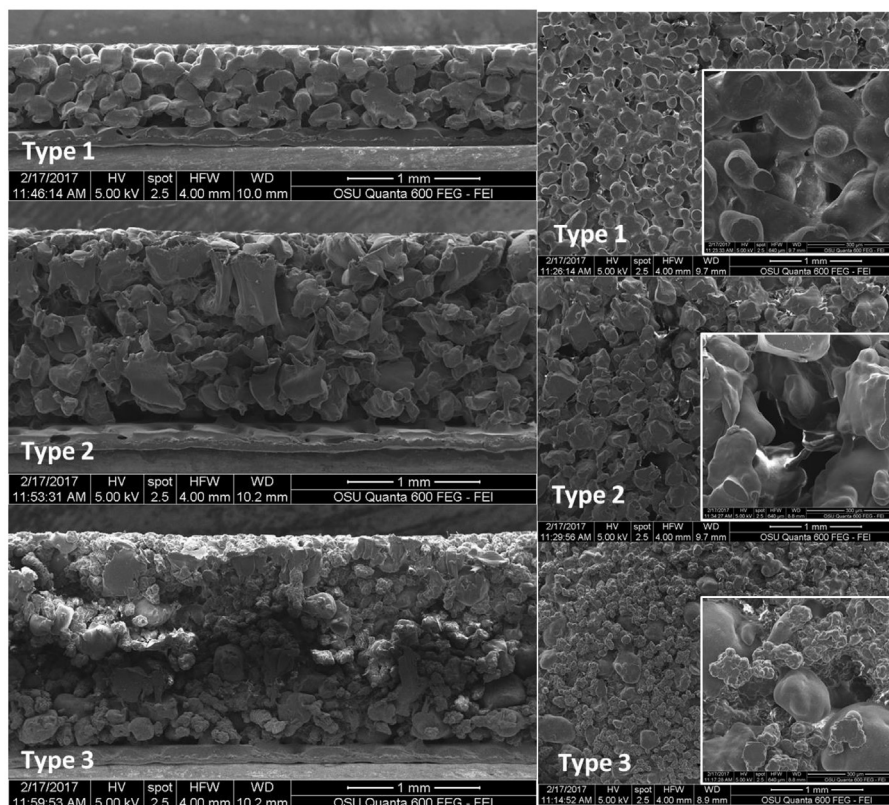
Fig. 2. SEM images of different PE sheets used in this study. Left: cross-section. Right: surface.

3.2. Electrochemical performance of PE cathodes with different AC/CB ratios

The electrochemical performance improves with the increased AC/CB ratio from 1:0.1 to 1:0.25 for type I PE cathode (Fig. 3), which is possibly due to the increased conductivity of the catalyst layer at higher CB loadings. Similar current densities were observed for the cathodes with AC/CB ratios of 1:0.5 and 1:0.25 within the typical MFC cathode potential range of 0—0.1 V (vs Ag/AgCl). The current densities are also comparable to the PTFE-CC cathode at the same AC loading of 25 mg cm^{-2}. This result suggests that carbon cloth current collector can be replaced with a more conductive catalyst layer without scarifying the electrochemical performance. Further increase of the AC/CB ratio to 1:1 resulted in lower current density. Since the AC loading remains the same in this study, the relatively low performance of 1:1 cathode is probably due to the much thicker catalyst layer that hinders the proton transfer on the cathode.

EIS analysis demonstrated that the ohmic resistance (R_o) of the PE cathode with 1:0.5 AC/CB ratio was about 72% of that PTFE-CC cathode (Fig. 4 and Table 2), indicating a better surface conductivity [44] of the PE cathode. Diffusion resistance (R_d) and Warburg impedance (W) are typically related to reactant diffusion on electrode [48,49]. The decreased R_d (22%) and W (66%) compared with the PTFE-CC cathode were possibly due to the faster oxygen diffusion in the PE cathode with larger pore size and the lack of carbon
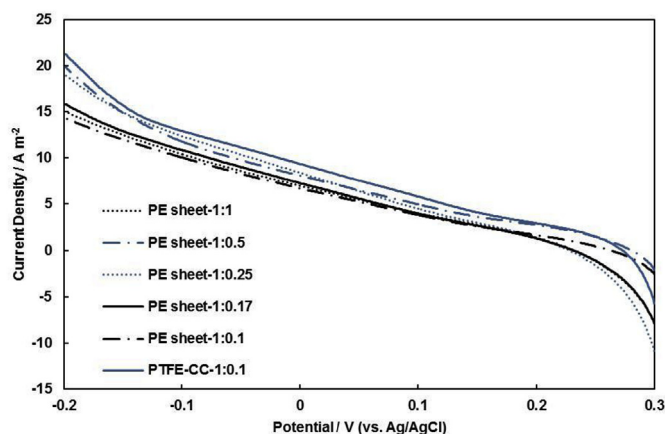

Fig. 3. Performance of type I PE cathodes with different AC/CB ratios.
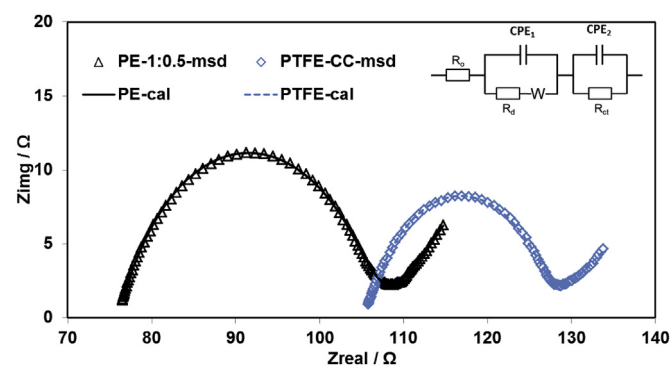

Fig. 4. Nyquist plots of EIS on different cathodes. Insertion: equivalent circuit model used in this study.

Table 2
Fitting results of different cathodes based on the equivalent circuit model in Fig. 4.

elements	PE-1:0.5	PTFE-CC
R_o/Ω	75.2	104.0
CPE_1-Q_1/Ω^{-1} sec^n	1.83×10^{-2}	4.25×10^{-2}
CPE_1-n_1	0.308	0.201
R_d/Ω	9.70	12.5
W/Ω $sec^{-0.5}$	9.40	27.6
CPE_2-Q_2/Ω^{-1} sec^n	4.42×10^{-5}	5.74×10^{-5}
CPE_2-n_2	0.835	0.851
R_{ct}/Ω	26.3	18.8

cloth layer. The charge transfer resistance (R_{ct}), which mainly reflects the reaction kinetics of the catalyst, however, increased by 40% in the PE cathodes. This increase could be due to the addition of CB, which increases the thickness of catalyst layer and isolates the AC catalyst particles. Constant phase element (CPE) is related to the double-layer capacitance of the electrode surface and bulk solution interface (CPE_1) and the interface of the electrode and solution in the electrode (CPE_2). The CPE consists of 2 parts: the numerical value Q, and the exponent n. (Fig. 4 insertion). The capacitance (Q_1 and Q_2) of the PE cathode were lower compared with the PTFE cathode possible due to a smaller actual surface area. The n_1 values of both materials are close to 0, indicating a more resistive behavior; while n_2 values are close to 1, showing a more capacitive behavior and relative smoother surface of both materials [50]. This new cathode decreased the internal resistance notably, though the cathode reaction kinetics is reduced.

3.3. Performance of MFCs with PE cathodes

Due to the better electrochemical performance of the PE cathode with type I PE sheet at AC/CB ratio of 1:0.5 and 1:0.25, these cathodes were selected and tested in MFCs. The MFCs started to produce repeatable power (~1.4 W m^{-2}) from day 15 at an external resistance of 130 Ω (Fig. 5a), which is similar to the MFCs with PTFE-CC cathodes (Figure S2). When evaluating the PTFE-CC and PE cathodes in the MFCs, the PTFE-CC cathodes generated a maximum power density of 1.2 to 1.0 W m^{-2} during about 1 month operation. After switching to the PE cathode, the max power densities increased to 1.4 W m^{-2} and maintained in the range of 1.4–1.1 W m^{-2} over the two-month operation (Fig. 5b). The
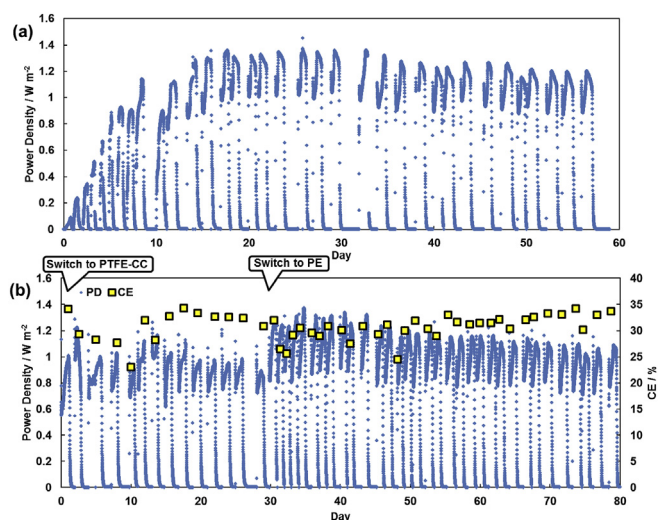
Fig. 5. (a) MFC started up with type I PE cathode (AC/CB ratio of 1:0.25), (b) Power densities and CEs of the MFC with type I PE cathode (AC/CB ratio of 1:0.5).

experiments were done in duplicate and similar results were obtained (Figure S3a and b). The enhanced power density in MFCs was possibly due to the larger pore size of the PE sheet compared with the PTFE layer [60]. This larger pore size could increase the oxygen transfer to the catalyst layer. This is particular the case in single-chambered MFCs, in which bacterial cells and their metabolites can potentially block the passage of oxygen in to the bulk solution. CEs of the MFCs maintain at a similar level after the replacement of the cathodes.

Maintaining the stability of cathode performance is critical for the practical application of MFCs. About 50% decrease in max power density has been observed in MFCs with Pt cathode and stainless steel mesh current collector within 1–3.5 month operation [51–55]. Using CC as the current collector can slow down the Pt cathode aging. However, up to 24% decrease within 2 months and 40% decrease in a year were still observed using acetate as carbon source [51–55]. Kim et al. also reported decrease in current density as high as 32% within one month using AC-PVDF cathodes fed by wastewater [56]. In this study, we observed 15% power decrease after two-month operation. Further testing on the long term stability of this PE cathode, especially using real wastewater is needed.

3.4. Simulation of ohmic potential drop during scaling up

Due to the intrinsic ohmic resistance, electrode materials can cause potential drop while the electrons are transferred from the connecting terminal to the catalyst activation sites within the cathode [18,47]. Most lab scale MFC studies didn't take this potential drop into account since the size of the electrode is too small, and other factors may play a more important role, such as mass transfer and electrolyte conductivity [18]. However, with the increased size of the electrode, the total electron transfer distance from the terminal to the catalytic sites also increases, causing a non-negligible ohmic potential drop due to the material ohmic resistance [47].

Fig. 6a shows six different terminal designs that were used for simulation. Fig. 6b to d shows the simulated potential drops of the designs at PE cathode scales of 0.1 m × 0.1 m, 0.5 m × 0.5 m, and 1 m × 1 m, respectively. One-point terminal connection (design 1, Fig. 6a) has only one inflow point as terminal located at the middle of the cathode edge, which is typically used in small-scale reactors. At small scale of 0.1 m × 0.1 m, this terminal connection could cause 0.02 V of potential drop. This is less than 6% of a normal MFC voltage output (~0.35 V), indicating that at this cathode scale, the potential drop caused by electrode material is not significant. With the expansion of cathode scale to 0.5 m × 0.5 m, the potential drop increases to 0.6 V with terminal design 1 (Fig. 6c). This potential drop exceeds the voltage that an MFC can generate, indicating that with this design, an MFC is not possible to reach the assumed current density of 3 A m^{-2} [47]. Adding connecting terminals using design 2 and 3 can effectively reduce the potential drop to 0.15 V and 0.04 V. This suggests that electrode resistance at the scale of 0.5 m × 0.5 m can result in notable potential drop, thus other terminal designs should be considered.

At a larger scale of 1 m × 1 m, terminal design 1 causes a considerable potential drop of 2.5 V (Fig. 6d). Using connecting terminal designs 2 to 5 can decrease the potential drop to 0.6 V, 0.15 V, 0.08 V and 0.08 V respectively, because of the distributed electron flow that reduces the total electron transfer routes and remits the potential drop accordingly. Two parallel terminals that are located at ¼ and ¾ of the cathode edge (design 6, Fig. 6a) could achieve the lowest potential drop of 0.04 V. This demonstrates that by using a two-parallel terminal design, the potential drop of the PE cathode can be reduced significantly. Further addition of
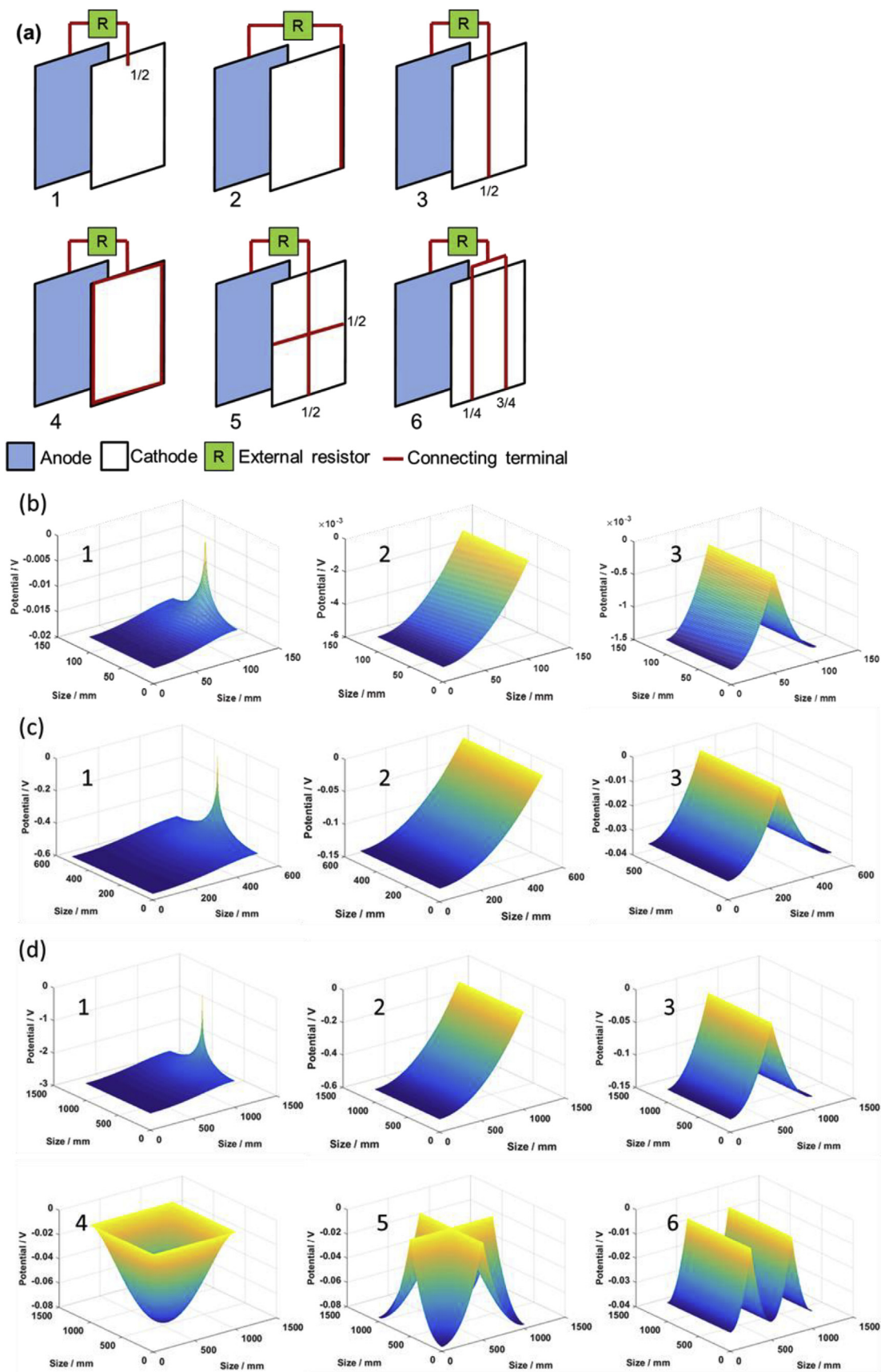
Fig. 6. (a) Different connecting terminal designs and the simulated potential drops of cathode size (b) 0.1 m × 0.1 m, (c) 0.5 m × 0.5 m and (d) 1 m × 1 m.

Table 3
Typical air-cathodes fabrication and current densities.

GDL type	current collector/supporting layer	solvent	curing temp. and time	current density at 0 V (v.s. Ag/AgCl)	refs.
Porous PE sheet	No	No	No	8.4 A m^{-2}	this study
PTFE emulsion	CC	No	370 °C, 40 min	Up to 10 A m^{-2}	[33,37] [a]
CB + PTFE rolling	SSM	No	340 °C, 1.5 h	6.6 A m^{-2}	[4,41]
PDMS solution	SSM	Toluene	80 °C, 5 h	~6 A m^{-2}	[38] [a]
PVDF solution	SSM	DMAc	Air-dry, 6 h	~3 A m^{-2}	[39]
GORE-TEX	PVC tube	No	No	~0.5 A m^{-2}	[40,42] [b]
PVDF membrane	SSM	Ethanol	60 °C (hot press), 15s	~5 A m^{-2}	[43]

[a] Indicates using Pt as catalyst.
[b] Indicates using MnO_2 as catalyst, and all others using AC as catalyst (loading 25–27 mg cm^{-2}).

connecting terminals can decrease the potential drop even further (Figure S4).

3.5. Potential of the PE cathode for practical applications

The PE cathode developed in this study greatly simplifies the fabrication procedure by directly applying the catalyst layer onto the PE sheet without solvent and current collector. It also substantially reduces the fabrication duration and energy needed for cathode fabrication.

Table 3 lists the materials and fabrication procedures of some commonly used MFC air-cathodes with activated carbon as catalyst. The porous PE sheet GDL achieved the highest current density among other GDLs except the PTFE emulsion. While many studies have suggested that the cathodes with PTFE as GDL can achieve high performance [57], long duration and high energy requirement are the main drawbacks for fabricating this material. Rolling method that uses a roller machine to heat and knead the carbon and PTFE mixture, can reduce the number of repeated coatings, but still need a high curing temperature of 340 °C after the rolling process [4]. PDMS and PVDF can be cured at low temperature of less than 80 °C, yet they require solvents such as toluene and DMAc, which add extra cost to the fabrication [38,39]. Hot pressing PVDF membrane can be less time-consuming, but generated only half of the current density of PTFE emulsion GDL [43].

Chemical fuel cells such as proton exchange membrane fuel cell (PEMFC) use carbon cloth/carbon paper as the base material of GDL. They also require a current collector, such as graphite plate to conduct the high electrical current and to provide mechanical strength to withstand the vibration [58,59]. Conductive metal mesh, such as stainless steel and nickel mesh have been used as current collector in MFC cathode. However, corrosion was observed in some studies possibly due to low oxygen environment or insufficient electron flow during the startup [36]. Since the current density of MFCs is typically less than 1% of a PEMFC, the necessity for a conductive current collector for MFC cathode largely depends on the size and design of electrode connection. At small scale (0.1 m × 0.1 m), the potential drop is not significant. This size might be sufficient for certain applications, such as small electronic devices and sensors. However, with the increased scale (e.g. 1 m × 1 m), the potential drop is significant with one-point connection. This drop, however, can be decreased to an acceptable level through proper terminal design, such as two-parallel terminal. Further increase of connection points might be undesirable since they may complicate the overall reactor fabrication. The contact resistance between the terminal and the catalyst layer may also increase the chance of potential drop.

High capital cost, mainly due to the high cost of cathode material, is still the major hurdle for the commercial application of MFCs. The cathode cost with Pt catalyst is estimated to be over $1000 m^{-2}. By replacing Pt with activated carbon and replacing Nafion with PTFE as binder, the cathode cost can be reduced to about $50-100 m^{-2}. However, this cost is still too high for MFCs with large electrode surface area to volume ratio, which is critical for the performance of MFC systems. By using PE, not only the fabrication cost can be greatly reduced, but the need for the expensive carbon cloth ($30-80 m^{-2}) can be eliminated. With a low raw material cost ($1 kg^{-1} polyethylene) and potential low fabrication cost for PE sheet, we expect that the total PE sheet cost can be less $5 m^{-2} and the total cost of the new PE based cathode can be less than $10 m^{-2}, which will completely eliminate the hurdle associated with cathode cost.

4. Conclusion

In this study, a new air cathode material that uses rigid and porous polyethylene sheet as gas diffusion layer and mechanical support was developed for the first time. Current collector was eliminated in this cathode by blending carbon black into the catalyst layer. This PE cathode achieved a more stable and better performance than the typical PTFE air cathodes in MFCs. The decent performance, the simplified procedure for fabrication, the low cost of the polyethylene material, and the low potential drop at larger scale suggest that this PE-based cathode has great potential for bulk manufacture, therefore speeding up the scaling up and practical application of MFC technology.

Appendix A. Supplementary data

Supplementary data related to this article can be found at https://doi.org/10.1016/j.energy.2018.05.055.

References

[1] McCarty PL, Bae J, Kim J. Domestic wastewater treatment as a net energy producer—can this be achieved? Environ Sci Technol 2011;45:7100–6. https://doi.org/10.1021/es2014264.

[2] Liu H, Logan BE. Electricity generation using an air-cathode single chamber microbial fuel cell in the presence and absence of a proton exchange membrane. Environ Sci Technol 2004;38:4040–6. https://doi.org/10.1021/es0499344.

[3] Fan Y, Hu H, Liu H. Enhanced Coulombic efficiency and power density of air-cathode microbial fuel cells with an improved cell configuration. J Power Sources 2007;171:348–54. https://doi.org/10.1016/j.jpowsour.2007.06.220.

[4] Dong H, Yu H, Wang X, Zhou Q, Feng J. A novel structure of scalable air-cathode without Nafion and Pt by rolling activated carbon and PTFE as catalyst layer in microbial fuel cells. Water Res 2012;46:5777–87. https://doi.org/10.1016/j.watres.2012.08.005.

[5] Ren H, Lee H-S, Chae J. Miniaturizing microbial fuel cells for potential portable power sources: promises and challenges. Microfluid Nanofluidics 2012;13:353–81. https://doi.org/10.1007/s10404-012-0986-7.

[6] Morris JM, Jin S, Crimi B, Pruden A. Microbial fuel cell in enhancing anaerobic

biodegradation of diesel. Chem Eng J 2009;146:161–7. https://doi.org/10.1016/j.cej.2008.05.028.

[7] Oh S, Min B, Logan BE. Cathode performance as a factor in electricity generation in microbial fuel cells. Environ Sci Technol 2004;38:4900–4. https://doi.org/10.1021/es049422p.

[8] You S, Zhao Q, Zhang J, Jiang J, Zhao S. A microbial fuel cell using permanganate as the cathodic electron acceptor. J Power Sources 2006;162:1409–15. https://doi.org/10.1016/j.jpowsour.2006.07.063.

[9] Lay C-H, Kokko ME, Puhakka JA. Power generation in fed-batch and continuous up-flow microbial fuel cell from synthetic wastewater. Energy 2015;91:235–41. https://doi.org/10.1016/j.energy.2015.08.029.

[10] Jang JK, Pham TH, Chang IS, Kang KH, Moon H, Cho KS, Kim BH. Construction and operation of a novel mediator- and membrane-less microbial fuel cell. Process Biochem 2004;39:1007–12. https://doi.org/10.1016/S0032-9592(03)00203-6.

[11] Moon H, Chang IS, Jang JK, Kim BH. Residence time distribution in microbial fuel cell and its influence on COD removal with electricity generation. Biochem Eng J 2005;27:59–65. https://doi.org/10.1016/j.bej.2005.02.010.

[12] Deng Q, Li X, Zuo J, Ling A, Logan BE. Power generation using an activated carbon fiber felt cathode in an upflow microbial fuel cell. J Power Sources 2010;195:1130–5. https://doi.org/10.1016/j.jpowsour.2009.08.092.

[13] Lu M, Chen S, Babanova S, Phadke S, Salvacion M, Mirhosseini A, Chan S, Carpenter K, Cortese R, Bretschger O. Long-term performance of a 20-L continuous flow microbial fuel cell for treatment of brewery wastewater. J Power Sources 2017;356:274–87. https://doi.org/10.1016/j.jpowsour.2017.03.132.

[14] Kim JR, Jung SH, Regan JM, Logan BE. Electricity generation and microbial community analysis of alcohol powered microbial fuel cells. Bioresour Technol 2007;98:2568–77. https://doi.org/10.1016/j.biortech.2006.09.036.

[15] Zinadini S, Zinatizadeh AA, Rahimi M, Vatanpour V, Rahimi Z. High power generation and COD removal in a microbial fuel cell operated by a novel sulfonated PES/PES blend proton exchange membrane. Energy 2017;125:427–38. https://doi.org/10.1016/j.energy.2017.02.146.

[16] Cheng S, Liu H, Logan BE. Power densities using different cathode catalysts (Pt and CoTMPP) and polymer binders (nafion and PTFE) in single chamber microbial fuel cells. Environ Sci Technol 2006;40:364–9. https://doi.org/10.1021/es0512071.

[17] Liu H, Ramnarayanan R, Logan BE. Production of electricity during wastewater treatment using a single chamber microbial fuel cell. Environ Sci Technol 2004;38:2281–5. https://doi.org/10.1021/es034923g.

[18] Fan Y, Sharbrough E, Liu H. Quantification of the internal resistance distribution of microbial fuel cells. Environ Sci Technol 2008;42:8101–7. https://doi.org/10.1021/es801229j.

[19] Fan Y, Han S-K, Liu H. Improved performance of CEA microbial fuel cells with increased reactor size. Energy Environ Sci 2012;5:8273. https://doi.org/10.1039/c2ee21964f.

[20] Zhang X, Cheng S, Wang X, Huang X, Logan BE. Separator characteristics for increasing performance of microbial fuel cells. Environ Sci Technol 2009;43:8456–61. https://doi.org/10.1021/es901631p.

[21] Salar-García MJ, Ortiz-Martínez VM, Baicha Z, de los Ríos AP, Hernández-Fernández FJ. Scaled-up continuous up-flow microbial fuel cell based on novel embedded ionic liquid-type membrane-cathode assembly. Energy 2016;101:113–20. https://doi.org/10.1016/j.energy.2016.01.078.

[22] Dekker A, Heijne AT, Saakes M, Hamelers HVM, Buisman CJN. Analysis and improvement of a scaled-up and stacked microbial fuel cell. Environ Sci Technol 2009;43:9038–42. https://doi.org/10.1021/es901939r.

[23] Zhuang L, Zhou S, Wang Y, Liu C, Geng S. Membrane-less cloth cathode assembly (CCA) for scalable microbial fuel cells. Biosens Bioelectron 2009;24:3652–6. https://doi.org/10.1016/j.bios.2009.05.032.

[24] Jiang D, Curtis M, Troop E, Scheible K, McGrath J, Hu B, Suib S, Raymond D, Li B. A pilot-scale study on utilizing multi-anode/cathode microbial fuel cells (MAC MFCs) to enhance the power production in wastewater treatment. Int J Hydrogy Energy 2011;36:876–84. https://doi.org/10.1016/j.ijhydene.2010.08.074.

[25] Wu C-H, Liu S-H, Chu H-L, Li Y-C, Lin C-W. Feasibility study of electricity generation and organics removal for a molasses wastewater by a waterfall-type microbial fuel cell. J Taiwan Inst Chem Eng 2017;78:150–6. https://doi.org/10.1016/j.jtice.2017.05.019.

[26] Zhuang L, Yuan Y, Wang Y, Zhou S. Long-term evaluation of a 10-liter serpentine-type microbial fuel cell stack treating brewery wastewater. Bioresour Technol 2012;123:406–12. https://doi.org/10.1016/j.biortech.2012.07.038.

[27] Ge Z, Zhang F, Grimaud J, Hurst J, He Z. Long-term investigation of microbial fuel cells treating primary sludge or digested sludge. Bioresour Technol 2013;136:509–14. https://doi.org/10.1016/j.biortech.2013.03.016.

[28] Zinadini S, Zinatizadeh AA, Rahimi M, Vatanpour V, Bahrami K. Energy recovery and hygienic water production from wastewater using an innovative integrated microbial fuel cell–membrane separation process. Energy 2017;141:1350–62. https://doi.org/10.1016/j.energy.2017.11.057.

[29] Salar-García MJ, Ortiz-Martínez VM, de los Ríos AP, Hernández-Fernández FJ. A method based on impedance spectroscopy for predicting the behavior of novel ionic liquid-polymer inclusion membranes in microbial fuel cells. Energy 2015;89:648–54. https://doi.org/10.1016/j.energy.2015.05.149.

[30] Kim JR, Cheng S, Oh S-E, Logan BE. Power generation using different cation, anion, and ultrafiltration membranes in microbial fuel cells. Environ Sci Technol 2007;41:1004–9. https://doi.org/10.1021/es062202m.

[31] He W, Zhang X, Liu J, Zhu X, Feng Y, Logan BE. Microbial fuel cells with an integrated spacer and separate anode and cathode modules. Environ Sci Water Res Technol 2016;2:186–95. https://doi.org/10.1039/C5EW00223K.

[32] Zhang F, Cheng S, Pant D, Bogaert GV, Logan BE. Power generation using an activated carbon and metal mesh cathode in a microbial fuel cell. Electrochem Commun 2009;11:2177–9. https://doi.org/10.1016/j.elecom.2009.09.024.

[33] Janicek A, Gao N, Fan Y, Liu H. High performance activated carbon/carbon cloth cathodes for microbial fuel cells. Fuel Cell 2015;15:855–61. https://doi.org/10.1002/fuce.201500120.

[34] Zuo Y, Cheng S, Logan BE. Ion exchange membrane cathodes for scalable microbial fuel cells. Environ Sci Technol 2008;42:6967–72. https://doi.org/10.1021/es801055r.

[35] Liu J, Feng Y, Wang X, Yang Q, Shi X, Qu Y, Ren N. The effect of water proofing on the performance of nickel foam cathode in microbial fuel cells. J Power Sources 2012;198:100–4. https://doi.org/10.1016/j.jpowsour.2011.09.078.

[36] Janicek A, Fan Y, Liu H. Performance and stability of different cathode base materials for use in microbial fuel cells. J Power Sources 2015;280:159–65. https://doi.org/10.1016/j.jpowsour.2015.01.098.

[37] Cheng S, Liu H, Logan BE. Increased performance of single-chamber microbial fuel cells using an improved cathode structure. Electrochem Commun 2006;8:489–94. https://doi.org/10.1016/j.elecom.2006.01.010.

[38] Zhang F, Saito T, Cheng S, Hickner MA, Logan BE. Microbial fuel cell cathodes with poly(dimethylsiloxane) diffusion layers constructed around stainless steel mesh current collectors. Environ Sci Technol 2010;44:1490–5. https://doi.org/10.1021/es903009d.

[39] Yang W, He W, Zhang F, Hickner MA, Logan BE. Single-step fabrication using a phase inversion method of poly(vinylidene fluoride) (PVDF) activated carbon air cathodes for microbial fuel cells. Environ Sci Technol Lett 2014;1:416–20. https://doi.org/10.1021/ez5002769.

[40] Zhuang L, Feng C, Zhou S, Li Y, Wang Y. Comparison of membrane- and cloth-cathode assembly for scalable microbial fuel cells: construction, performance and cost. Process Biochem 2010;45:929–34. https://doi.org/10.1016/j.procbio.2010.02.014.

[41] Dong H, Yu H, Wang X. Catalysis kinetics and porous analysis of rolling activated carbon-PTFE air-cathode in microbial fuel cells. Environ Sci Technol 2012;46:13009–15. https://doi.org/10.1021/es303619a.

[42] Luo Y, Zhang F, Wei B, Liu G, Zhang R, Logan BE. The use of cloth fabric diffusion layers for scalable microbial fuel cells. Biochem Eng J 2013;73:49–52. https://doi.org/10.1016/j.bej.2013.01.011.

[43] Yang W, Logan BE. Engineering a membrane based air cathode for microbial fuel cells via hot pressing and using multi-catalyst layer stacking. Environ Sci Water Res Technol 2016. https://doi.org/10.1039/C6EW00098C.

[44] Wang X, Gao N, Zhou Q, Dong H, Yu H, Feng Y. Acidic and alkaline pretreatments of activated carbon and their effects on the performance of air-cathodes in microbial fuel cells. Bioresour Technol 2013;144:632–6. https://doi.org/10.1016/j.biortech.2013.07.022.

[45] Lovley DR, Phillips EJP. Novel mode of microbial energy metabolism: organic carbon oxidation coupled to dissimilatory reduction of iron or manganese. Appl Environ Microbiol 1988;54:1472–80.

[46] Liu H, Cheng S, Logan BE. Production of electricity from acetate or butyrate using a single-chamber microbial fuel cell. Environ Sci Technol 2005;39:658–62. https://doi.org/10.1021/es048927c.

[47] Cheng S, Ye Y, Ding W, Pan B. Enhancing power generation of scale-up microbial fuel cells by optimizing the leading-out terminal of anode. J Power Sources 2014;248:931–8. https://doi.org/10.1016/j.jpowsour.2013.10.014.

[48] He Z, Mansfeld F. Exploring the use of electrochemical impedance spectroscopy (EIS) in microbial fuel cell studies. Energy Environ Sci 2009;2:215–9. https://doi.org/10.1039/B814914C.

[49] You S, Zhao Q, Zhang J, Jiang J, Wan C, Du M, Zhao S. A graphite-granule membrane-less tubular air-cathode microbial fuel cell for power generation under continuously operational conditions. J Power Sources 2007;173:172–7. https://doi.org/10.1016/j.jpowsour.2007.07.063.

[50] Zhang F, Merrill MD, Tokash JC, Saito T, Cheng S, Hickner MA, Logan BE. Mesh optimization for microbial fuel cell cathodes constructed around stainless steel mesh current collectors. J Power Sources 2011;196:1097–102. https://doi.org/10.1016/j.jpowsour.2010.08.011.

[51] Zhang F, Pant D, Logan BE. Long-term performance of activated carbon air cathodes with different diffusion layer porosities in microbial fuel cells. Biosens Bioelectron 2011;30:49–55. https://doi.org/10.1016/j.bios.2011.08.025.

[52] Wei B, Tokash JC, Chen G, Hickner MA, Logan BE. Development and evaluation of carbon and binder loading in low-cost activated carbon cathodes for air-cathode microbial fuel cells. RSC Adv 2012;2:12751–8. https://doi.org/10.1039/C2RA21572A.

[53] Xia X, Zhang F, Zhang X, Liang P, Huang X, Logan BE. Use of pyrolyzed iron ethylenediaminetetraacetic acid modified activated carbon as air–cathode catalyst in microbial fuel cells. ACS Appl Mater Interfaces 2013;5:7862–6. https://doi.org/10.1021/am4018225.

[54] Zhang X, Xia X, Ivanov I, Huang X, Logan BE. Enhanced activated carbon cathode performance for microbial fuel cell by blending carbon black. Environ Sci Technol 2014;48:2075–81. https://doi.org/10.1021/es405029y.

[55] Li D, Liu J, Wang H, Qu Y, Feng Y. Effect of long-term operation on stability and electrochemical response under water pressure for activated carbon cathodes in microbial fuel cells. Chem Eng J 2016;299:314–9. https://doi.org/10.1016/j.cej.2016.04.035.

[56] Kim K-Y, Yang W, Ye Y, LaBarge N, Logan BE. Performance of anaerobic fluidized membrane bioreactors using effluents of microbial fuel cells treating domestic wastewater. Bioresour Technol 2016;208:58—63. https://doi.org/10.1016/j.biortech.2016.02.067.

[57] Zhang X, He W, Yang W, Liu J, Wang Q, Liang P, Huang X, Logan BE. Diffusion layer characteristics for increasing the performance of activated carbon air cathodes in microbial fuel cells. Environ Sci Water Res Technol 2016;2:266—73. https://doi.org/10.1039/C5EW00245A.

[58] Mehta V, Cooper JS. Review and analysis of PEM fuel cell design and manufacturing. J Power Sources 2003;114:32—53. https://doi.org/10.1016/S0378-7753(02)00542-6.

[59] Park S, Popov BN. Effect of a GDL based on carbon paper or carbon cloth on PEM fuel cell performance. Fuel 2011;90:436—40. https://doi.org/10.1016/j.fuel.2010.09.003.

[60] Santoro C, Agrios A, Pasaogullari U, Li B. Effects of gas diffusion layer (GDL) and micro porous layer (MPL) on cathode performance in microbial fuel cells (MFCs). Int J Hydrogen Energy 2011;36:13096—104. https://doi.org/10.1016/j.ijhydene.2011.07.030.